Chemical Engineering Journal 373 (2019) 1072–1080

Contents lists available at ScienceDirect

Chemical Engineering Journal

journal homepage: www.elsevier.com/locate/cej

Resource recovery microbial fuel cells for urine-containing wastewater treatment without external energy consumption

Sidan Lu[a], Hongna Li[b], Guangcai Tan[a], Fang Wen[c], Michael T. Flynn[d], Xiuping Zhu[a,*]

[a] Department of Civil and Environmental Engineering, Louisiana State University, Baton Rouge, LA 70803, USA
[b] Agricultural Clean Watershed Research Group, Institute of Environment and Sustainable Development in Agriculture, Chinese Academy of Agricultural Sciences, Beijing 100081, China
[c] Xinjiang Academy of Environmental Protection Science, Urumqi, Xinjiang 830011, China
[d] NASA Ames Research Center, Moffett Field, CA 94035, USA

HIGHLIGHTS

- A resource recovery microbial fuel cell is proposed for urine-containing wastewater treatment.
- Urea hydrolysis rate is increased by microbial and electrical processes.
- Ammonium migration through the ion exchange membrane replaces ammonia stripping.
- N, P, and S nutrients are efficiently recovered.
- No external energy consumption is needed.

ARTICLE INFO

Keywords:
Urine-containing wastewater treatment
Bio-electrochemical systems
Resource recovery
Microbial fuel cell

ABSTRACT

Resources in urine-containing wastewater are useful if recovered as nutrients. In this study, a three-chamber resource recovery microbial fuel cell (RRMFC) is proposed to treat synthetic urine-containing wastewater with various organic pollutants and recover N, P, and S nutrients. In the treatment, urea hydrolysis was increased by microbial and electrical processes. Ions migration driven by the self-generated electric field was used to recover nutrients from the wastewater. Over one cycle (~3 days), 99% of urea, 97% of COD, 99% of histidine, 91% of creatinine, 99% of sodium acetate, 98% of SO_4^{2-}, and 99% of PO_4^{3-} were removed from the wastewater, and at the same time, 42% of total nitrogen, 37% of PO_4^{3-}, 59% of SO_4^{2-}, and 33% of total salts were recovered in the middle chamber. This technology is very attractive for sustainable resource recovery from urine-containing wastewater.

1. Introduction

Nitrogen pollution is a significant environmental issue around the world. Eutrophication causes a scarcity in usable water and increases the cost of water treatment [1]. Nowadays, nitrification and denitrification have been applied to remove ammonium and nitrate from wastewater [2]. However, urine is another big source of nitrogen pollution that is requiring more advanced treatment methods [3]. In domestic wastewater, urine comprises approximately 75–80% of the nitrogen but the volume only accounts for 1% of the total water [3]. Traditional techniques for urine-containing wastewater treatment required biological processes to hydrolyze urea [4]. The produced ammonium was sequentially removed via an ammonia striping column under the alkali condition [4,5] or converted into the precipitates of calcium phosphate minerals or struvite [6]. However, the efficiency of urea hydrolysis is usually low [7] and the ammonia stripping process is energy intensive [5]. Therefore, developing more effective and economic methods to treat urine-containing wastewater is in high demand [8]. On the other hand, urine-containing wastewater is a rich source of nitrogen (N), phosphorus (P), and sulfur (S) nutrients. Recovering resources from urine-containing wastewater would be helpful for pollution control and also benefit agriculture [9,10].

Bio-electrochemical systems (BESs) have been developed to treat wastewater and recover resources attributed to the abundant fuel sources, mild reaction conditions, and high efficiencies [11]. Microbial fuel cells (MFCs) is a typical type of BESs that use microbes as the

* Corresponding author.
E-mail address: xzhu@lsu.edu (X. Zhu).

https://doi.org/10.1016/j.cej.2019.05.130
Received 30 January 2019; Received in revised form 17 May 2019; Accepted 20 May 2019
Available online 20 May 2019

catalyst to remove organic pollutants from wastewater and produce electricity simultaneously [12]. Besides MFCs, many other BESs have been developed to utilize the generated electricity, such as microbial desalination cells (MDCs) to reduce salinity with an added desalination chamber between the anode and the cathode [13] and microbial electrolysis cells (MECs) that generate H_2 gas at the cathode with an additional small voltage (~1 V) [14]. BESs are also developed for urine treatment and resource recovery. In 2012, a communication reported for the first time the direct utilization of urine in MFCs for the production of electricity [15]. Later, nutrients separation microbial electrolysis cells (NSMECs) were introduced to concentrate ammonium and phosphate from diluted synthetic hydrolyzed urine, however the technique required an energy consumption of 0.44 kWh per m^3 [16]. Another research proposed that pre-treatment of BESs followed by membrane aeration successfully converted 80–90% of organic nitrogen into ammonium nitrogen [17]. The disadvantage is that the urine needed a pre-hydrolyzation before the treatments, which increased the complexity of the processes. To further facilitate urea hydrolysis, a stacked microbial nutrient recovery cell (SMNRC) was proposed with the self-generated field and harvested 76–87% of N and 72–93% of P from source-separated urine [18]. To save the energy of ammonia stripping, researchers coupled an alkalifying electrochemical cell for direct liquid-liquid extraction with a hydrophobic gas membrane to replace the conventional stripping column, and nitrogen recovery from urine was improved [8]. Moreover, interests in micro-pollutants and organics such as ethinylestradiol, diclofenac, and carbamazepine contained in human urine has also been considered [19,20].

In this study, a resource recovery microbial fuel cell (RRMFC) is designed to treat urine-containing wastewater with various organic and inorganic substrates and simultaneously recover nutrients and salts. In the RRMFC, a middle chamber was added between the anode and the cathode, a cation exchange membrane (CEM) was used to separate the middle chamber from the anode chamber, and an AEM was applied between the middle chamber and the cathode chamber. Driven by the self-generated electric field between the anode and the cathode, the cations migrated from the anode chamber to the middle chamber through the CEM and the anions moved from the cathode chamber to the middle chamber through the AEM. As a result, N, P, and S nutrients were separated from the wastewater and concentrated in the middle chamber without external energy consumption. Additionally, urea hydrolysis was enhanced in the anode chamber by electrical and biological processes, and ammonium was recovered by the ion migration process instead of using energy-intensive ammonia stripping.

2. Materials and methods

2.1. Configuration of RRMFC reactors

An RRMFC contained three chambers with cylindrical configurations inside polycarbonate cubes. The chambers were all 3 cm in diameter: an anode chamber (4 cm length, 28 mL), a middle chamber (2 cm length, 14 mL), and a cathode chamber (4 cm length, 28 mL) (Fig. 1). A cation exchange membrane (CEM, Selemion CMV) was placed between the anode chamber and the middle chamber, while an anion exchange membrane (AEM, Selemion AMV) was added between the middle chamber and the cathode chamber. The anode was a graphite fiber brush (2.5 cm in diameter × 2.5 cm in length), which was heated at 450 °C for 30 min in a muffle furnace (ThermoFisher Scientific) to gain a higher N/C ratio and a lower C–O composition [21]. The cathode was an circular activated carbon air–cathode (7 cm^2), which was made by a phase inversion method [22].

2.2. Operation of RRMFC reactors

The carbon brush anode was preacclimated with electroactive microbes in a single-chamber MFC with a cylindrical configuration (3 cm in diameter, 4 cm in length, and 28 mL in volume) inside a polycarbonate cube and an activated carbon air-cathode. The MFC was inoculated with a 50:50 (v/v) mixture of anaerobic digestion sludge and growth medium. The anaerobic digestion sludge was collected from the East Baton Rouge South Wastewater Treatment Plant (Baton Rouge, LA, US). The growth medium contained (per L): 1 g sodium acetate, 4.28 g Na_2HPO_4 2.45 g $NaH_2PO_4{\cdot}H_2O$, 0.31 g NH_4Cl, 0.13 g KCL, 12.5 mL minerals, and 5 mL vitamins [23]. After incubated for 3 days in a 30 °C thermotank (ThermoFisher Scientific, US), electricity was generated. Later, only the growth medium was fed to the MFC for at least 30 cycles (1 day per cycle) until the current was stable (Fig. 2, inserted figure). Then, the carbon brush anode was transferred into the anode chamber of the RRMFC for urine-containing wastewater treatment.

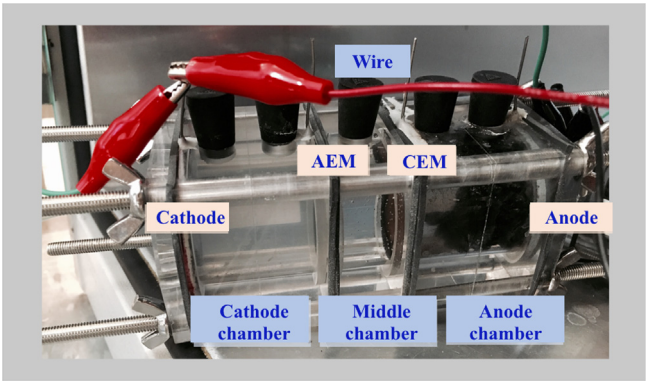

Fig. 1. Configuration of the resource recovery microbial fuel cell (RRMFC).

The RRMFC was operated in a batch mode (3 days per cycle) in a 30 °C thermotank (ThermoFisher Scientific, US). The batch operation mode was chosen mainly considering the simple reactor design and operations. The anode chamber of the RRMFC was fed with 23 mL synthetic urine-containing wastewater with a 10-times diluted urine concentration, which was similar to raw urine after toilet flushing [7]. The synthetic wastewater contained (per L): 1717 mg urea, 1000 mg sodium acetate, 90 mg creatinine, 142 mg histidine, 507 mg NaCl, 135 mg K_2SO_4, 132 mg KH_2PO_4, 72 mg $MgCl_2{\cdot}6H_2O$, 22 mg NH_4HCO_3, 48 mg $CaCl_2{\cdot}2H_2O$, and 193 mg KCl. The cathode chamber of the RRMFC was supplied with the effluent of the anode chamber from last cycle, which was held in the cathode chamber for one cycle (3 days). The middle chamber was fed with deionized water for the purpose of nutrient recovery. Graduated syringes were used to feed and suck out all solutions from the three chambers to avoid leaving behind residuals from the last cycle and measure the real water volumes. A relatively small external resistance of 10 Ω was connected between the anode and the cathode to monitor the current based on Ohm's law (I = U/R) and simultaneously allowed for a high current generation compared to larger resistances. At the end, a control reactor with the same configuration as the RRMFC without sterilization was run under an open circuit condition to distinguish the effects of the self-generated electric field on ions migration. The sterilized control reactor was not considered here because wastewaters always contain microbes.

2.3. Chemical analysis

To analyze the performance of the RRMFC reactor, the input and output of each chamber were monitored. Water samples were taken separately from each chamber at the beginning and the end of every fed-batch cycle (~3 days). The samples were filtered through 0.22 um syringe filters (PVDF, Restek Corporation) before all chemical analysis. Phosphate, sulfate, nitrite, and ammonium ions were determined by SmartChem 170 (Unity Scientific, US) according to the United States Environmental Protection Agency (EPA) standard methods [24]. Nitrate and the soluble chemical oxygen demand (COD) were determined

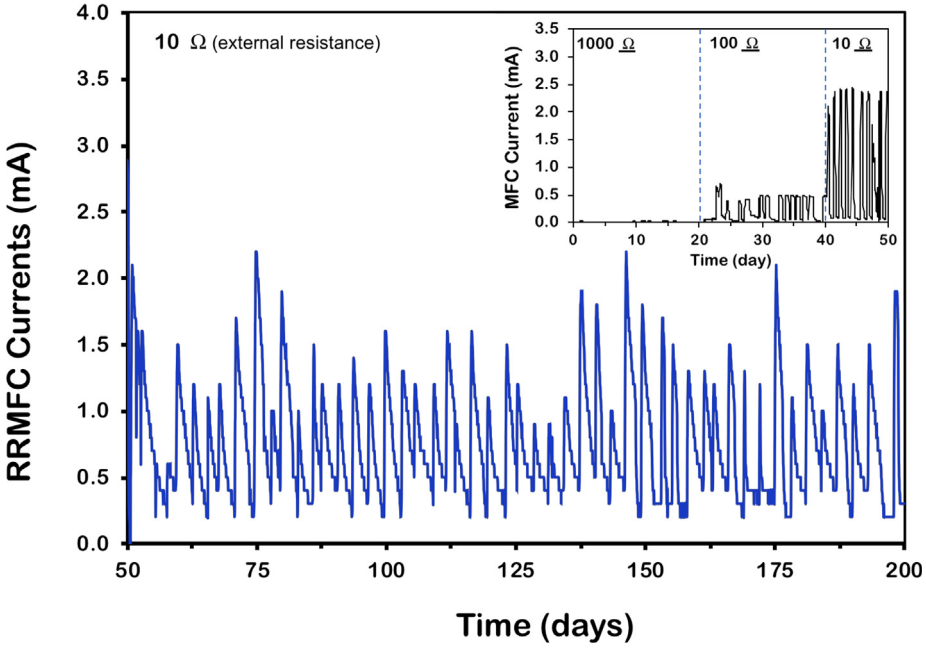

Fig. 2. Currents of the MFC and the resource recovery microbial fuel cell (RRMFC) with different external resistances. The main part shows the currents of the RRMFC, the magnified view (the smaller figure) showed the currents of the MFC. (The chemical analysis started from the 60th day).

using test kits (TNT plus vial test, Hach Co.). The pH of the solution was tested using a pH meter (VWR SB70P). Conductivity was measured using a conductivity meter (VWR SB90M5). Urea was analyzed by spectrophotometric method at 525 nm wavelength after digested in water bath with diacetylmonoxime at 95 °C [25]. Histidine, creatinine, and sodium acetate were detected by high performance liquid chromatography (HPLC) (Agilent 1260) with a C18 column (250 mm length) at a temperature of 30 °C and a UV detector at the wavelength of 205 nm. The injection volume to the HPLC was 5 uL, the mobile phase was acetonitrile and H_3PO_4 (10 mM) (7:93, v/v), and the flow rate was 0.2 mL/min.

2.4. Calculations

Due to adding of electrodes and membranes and withdrawing of samples, the real water volumes added in each chamber were different from the chamber volumes (that is, ~23 mL for the anode chamber, ~19 mL for the middle chamber, and ~19 mL for the cathode chamber). The effluent volumes of the anode and middle chambers were similar to the added volumes, but the effluent volumes of the cathode chamber decreased to ~5 mL due to evaporation from the air-cathode. Graduated syringes were used to measure the real water volumes in and out of each chamber for every cycle. The mass in and mass out were then calculated based on the concentration and the measured real water volumes. Average mass values over 33 cycles were reported with 95% confidence intervals. The removal efficiency (%) of each substance in the wastewater was calculated based on the average mass out of the cathode chamber over the average mass in of the anode chamber. The removal rates of each substance (g m^{-3} d^{-1}) were calculated as the average removed mass normalized to the cycle time (~3 days) and the volume of the anode and cathode chambers (56 mL). The recovery efficiency (%) of ions was obtained as the ratio between the average mass out of the middle chamber and the average mass in of the anode chamber. The total nitrogen recovery efficiency was calculated based on the total N mass out of the middle chamber (i.e., urea, NH_4^+, NO_3^-, and NO_2^-) over the total N mass in of the synthetic wastewater (urea and ammonium bicarbonate). The columbic efficiency was the ratio between the experimental coulombs by integrating the current over time and the theoretical coulombs calculated based on COD changes ($C_{theoretical} = F \bullet b \bullet V_{an} \bullet \Delta COD$, F is Faraday's constant, b = 4 indicates the number of electrons exchanged per mole of oxygen, V_{an} is the volume of liquid in the anode compartment, and ΔCOD is the change of the COD over time) [26].

3. Results and discussion

3.1. Electricity generation of the RRMFC

The anode of the RRMFC was preacclimated with electroactive microbes in a MFC. The maximum power density of the MFC was 1300 mW/m^2 with an open circuit voltage of 0.72 V and an internal resistance of 208 Ω (Fig. S1). The maximum current of the MFC was ~0.04 mA at an external resistance of 1000 Ω. The values increased to ~0.5 mA at 100 Ω and ~2.80 mA at 10 Ω (Fig. 2, inserted figure), which were comparable to previous studies on MFCs [27]. Then, the anode was transferred to the RRMFC. The maximum currents of the RRMFC varied within the range of 1.30 ± 0.30 mA at an external resistance of 10 Ω (Fig. 2), which was lower than that of the MFC as a combined result of the increased internal resistance from the addition of the middle chamber and the feed-solution change from growth media to urine-containing wastewater.

3.2. Chemical removal and recovery

After the current of the RRMFC became stable, the concentrations of urea, COD, histidine, creatinine, sodium acetate, ammonium, nitrite, nitrate, sulfate, phosphate, pH, and salinity in each chamber were monitored at the beginning and the end of each cycle for 33 cycles (~3 days per cycle) (Fig. 3). The mass in and out of each substance in each chamber were then calculated based on the concentration and the measured real solution volumes. The average mass in and out over the 33 cycles were shown in Fig. 4 and Table 1 with 95% confidence intervals. The removal and recovery efficiencies were then calculated based on the average mass in and out (Table 1). It should be noted that the mass balance on C, N, P, and S nutrients was difficult to be established because species turned into gases and solids were not monitored during the treatment, e.g., volatilization of some compounds, production of CO_2, CH_4, N_2 and NH_3 gases, and formation of struvite

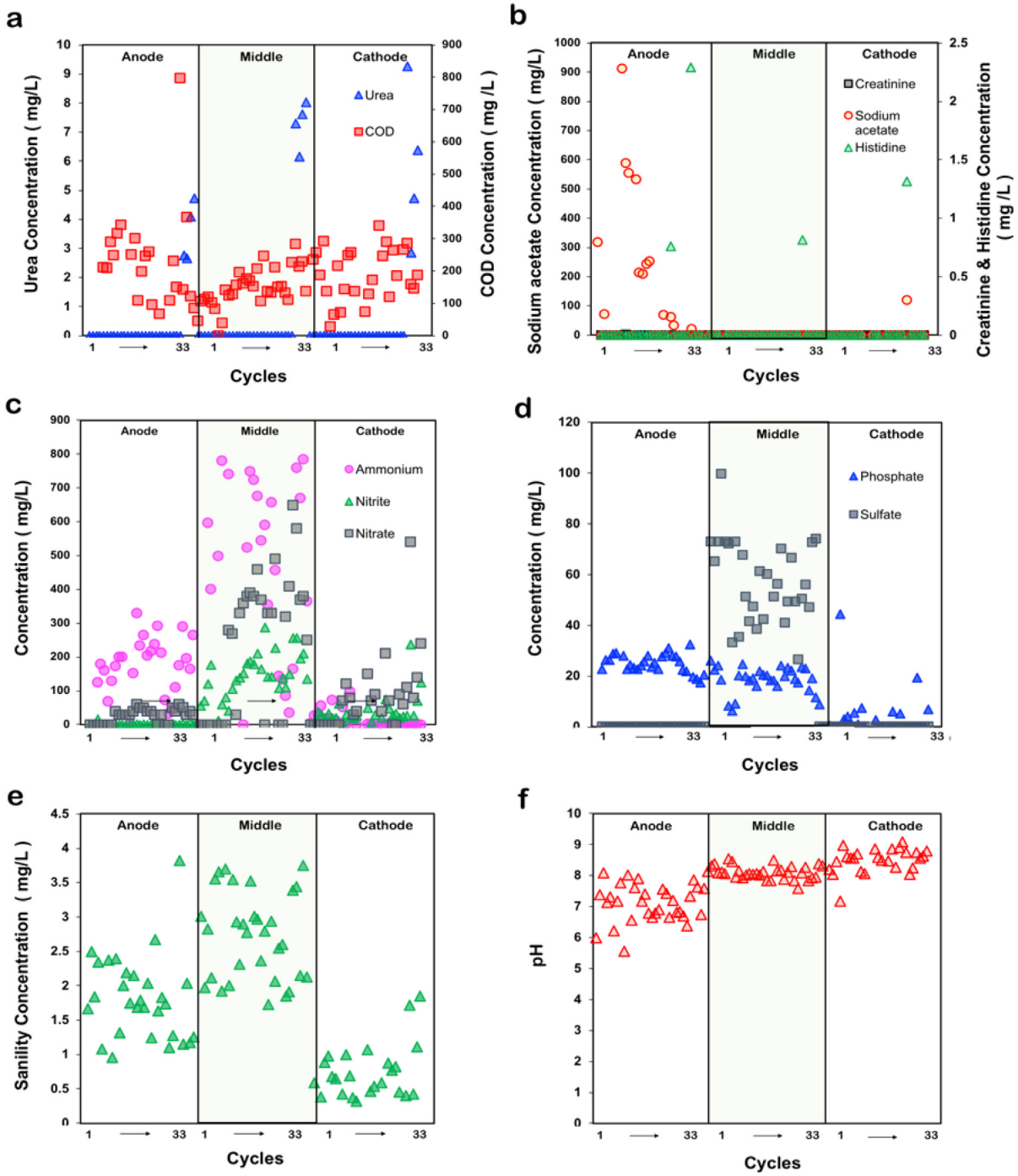

Fig. 3. Concentrations of (a) urea and COD, (b) histidine, creatinine, and sodium acetate, (c) ammonium, nitrite, and nitrate, (d) phosphate and sulfate, (e) salinity, and (f) pH in the anode, middle and cathode chambers of the resource recovery microbial fuel cell (RRMFC) at the end of 33 cycles.

precipitation and biomass.

3.2.1. Urea reduction and transfer

The urea decreased from 39.50 to 0.05 ± 0.05 mg in the anode chamber and further reduced to 0 mg in the cathode chamber with a removal efficiency of 99% and a removal rate of 235 g m^{-3} d^{-1} (Fig. 4a and Table 1). According to previous studies [28,29], urea can be hydrolyzed with urease that was synthesized by microbes widely distributing in soil and aquatic environments. Therefore, in the anode and cathode chambers of the RRMFC, urea was hydrolyzed and NH_3 gas was produced (Eq. (1)) [28]. The electric field also accelerated the urea hydrolyzing speed in the RRMFC according to previous studies [18]. As a result, most of urea was removed in the anode chamber (99%). The produced NH_3 from urea hydrolysis formed NH_4^+ that was further oxidized into NO_2^-, NO_3^-, or N_2 through nitrification or the Anammox processes [30]. Additionally, the increase of urea from 0 to 0.08 ± 0.02 mg in the middle chamber indicated that part of urea was transferred to the middle chamber because the AEM and CEM could not completely prevent urea from passing through the chambers.

3.2.2. Organics reduction and transfer

The COD decreased from 24.60 to 6.71 ± 1.39 mg in the anode chamber and further reduced to 0.74 ± 0.17 mg in the cathode chamber with a removal efficiency of 97% and a removal rate of

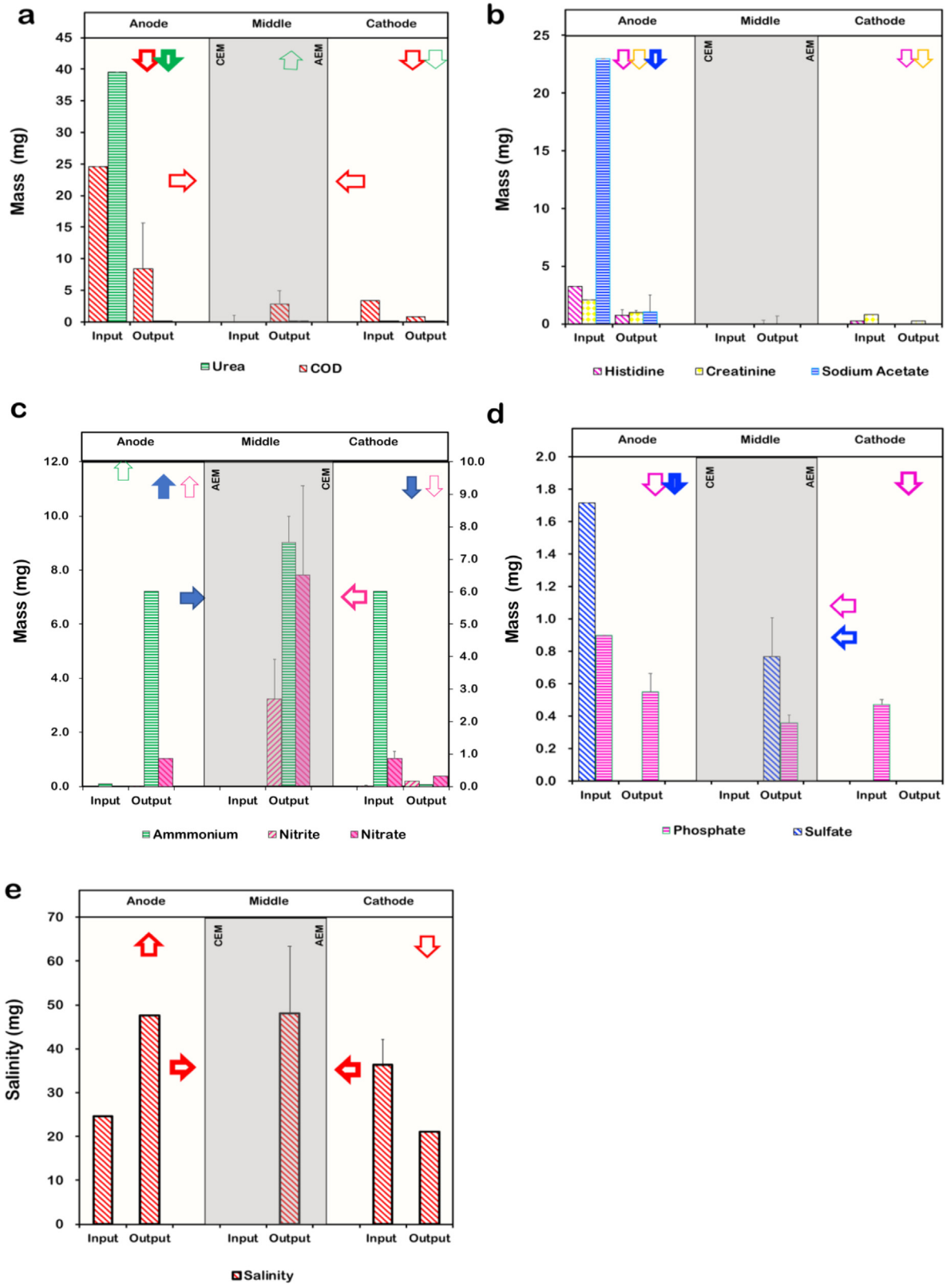

Fig. 4. Mass reduction and transfer graphic trends in the anode, middle, and cathode chambers of the resource recovery microbial fuel cell (RRMFC): (a) urea and COD, (b) histidine, creatinine, and sodium acetate, (c) ammonium, nitrite, and nitrate, (d) phosphate and sulfate, and (e) salinity. The up-arrows in the figure indicate the increase, the down-arrows indicate the decrease, and the horizontal-arrows indicate the ions transference. The line width of the arrows indicates the extent of the mass change.

Table 1
Chemical parameters characterizing the urine-containing wastewater treatment in the microbial recovery cell (the data range is based on 95% confidence intervals).

	Anode in (mg)	Anode out (mg)	Middle in (mg)	Middle out (mg)	Cathode in (mg)	Cathode Out (mg)	Removal (%)	Recovery (%)
Urea	39.50	0.05 ± 0.05	0	0.08 ± 0.02	0.05 ± 0.05	0	99	N/A
COD	24.60	6.71 ± 1.39	0	2.79 ± 0.45	6.71 ± 1.39	0.74 ± 0.17	97	N/A
Histidine	3.30	0.81 ± 0.01	0	0	0.81 ± 0.01	0	99	N/A
Creatinine	2.10	0.60 ± 0.01	0	0	0.60 ± 0.01	0.19 ± 0.02	91	N/A
Sodium acetate	23.00	0.95 ± 0.91	0	0	0.95 ± 0.91	0.02 ± 0.02	99	N/A
Ammonium	0.10	7.22 ± 0.81	0	9.01 ± 2.12	7.22 ± 0.81	0.06 ± 0.04	40	N/A
Nitrite	0	0	0	2.69 ± 0.51	0	0.17 ± 0.07	N/A	N/A
Nitrate	0	0.87 ± 0.18	0	6.51 ± 1.43	0.87 ± 0.18	0.32 ± 0.18	N/A	N/A
Total N	20.20	4.34 ± 1.96	0	9.44 ± 2.16	4.34 ± 1.96	0.27 ± 0.08	98	42
Sulfate	1.70	0	0	1.01 ± 0.15	0	0.04 ± 0.04	98	59
Phosphate	0.90	0.48 ± 0.08	0	0.33 ± 0.04	0.48 ± 0.08	0.02 ± 0.01	99	37
Salinity	24.60	46.04 ± 6.60	0	47.65 ± 7.01	46.04 ± 7.60	21.00 ± 4.10	15	33
pH	6.90	6.00–7.90	7.20	7.90–8.50	6.00–7.90	8.10–8.90	N/A	N/A

142 $g\,m^{-3}\,d^{-1}$ (Fig. 4a and Table 1). Most of organics was degraded in the anode chamber by microbes [26,31], which provided electrons to the external circuit to produce electricity with a columbic efficiency of 55%. Part of organics was removed in the cathode chamber via microbial processes. Additionally, there was 11% of organics transferred to the middle chamber as the COD in the middle chamber increased from 0 to 2.79 ± 0.45 mg.

The histidine decreased from 3.30 to 0.81 ± 0.01 mg in the anode chamber and further reduced to 0 mg in the cathode chamber (Fig. 4b). The removal efficiency of histidine was 99% (Table 1) with a removal rate of 20 $g\,m^{-3}\,d^{-1}$. The creatinine reduced from 2.10 to 0.6 ± 0.01 mg in the anode chamber and further decreased to 0.19 ± 0.02 mg in the cathode chamber (Fig. 4b). The removal efficiency of creatinine was 91% (Table 1) with a removal rate of 11 $g\,m^{-3}\,d^{-1}$. The sodium acetate decreased from 23.00 to 0.95 ± 0.91 mg in the anode chamber and was 0.02 ± 0.02 mg in the cathode chamber (Fig. 4b). The removal efficiency of sodium acetate was 99% (Table 1) and the removal rate reached 137 $g\,m^{-3}\,d^{-1}$. Histidine, creatinine, and sodium acetate were mainly degraded in the anode chamber and partly removed in the cathode chamber, but none of them were detected in the middle chamber. The detected COD in the middle chamber (Fig. 4a) indicated that some degradation intermediates of the organics transferred to the middle chamber. Further investigations are still needed to identify these intermediates.

3.2.3. Nitrogen reduction and transfer

As shown in Fig. 4c, the NH_4^+ mass increased from 0.10 to 7.22 ± 0.81 mg in the anode chamber over one cycle, which could be largely attributed to urea hydrolysis [32] as well as histidine and creatinine degradation [33]. The NH_4^+ mass in the middle chamber increased from 0 to 9.01 ± 2.12 mg (Fig. 4c), indicating that a large amount of NH_4^+ was transferred from the anode chamber to the middle chamber through the CEM. In the cathode chamber, the NH_4^+ decreased from 7.22 to 0.06 ± 0.04 mg (Fig. 4c), which could be attributed to the nitrification process conducted by ammonia oxidizing and nitrifying microbes [34]. Additionally, NH_4^+ could also be oxidized to N_2 through the Anammox process (Eq. (4)) [35,36].

The NO_3^- mass increased from 0 to 0.87 ± 0.08 mg in the anode chamber (Fig. 4c), which should be due to the oxidation of NH_4^+ [30]. The NO_3^- mass in the cathode chamber decreased from 0.87 to 0.32 ± 0.18 mg (Fig. 4c), indicating that NO_3^- moved from the cathode chamber to the middle chamber through the AEM. As a result, the NO_3^- mass in the middle chamber increased from 0 to 6.51 ± 1.43 mg (Fig. 4c). However, the increased NO_3^- mass (6.51 mg) in the middle chamber was much larger than the decreased NO_3^- mass (0.55 mg) in the cathode chamber, indicating that more NO_3^- was produced in the cathode chamber by the nitrification process of NH_4^+.

The NO_2^- was not observed in the anode chamber, while the NO_2^- mass increased from 0 to 2.69 ± 0.51 mg in the middle chamber and from 0 to 0.17 ± 0.07 mg in the cathode chamber (Fig. 4c). Similar to NO_3^-, the increase in the cathode chamber could be due to the nitrification of NH_4^+ to NO_2^-. Moreover, the rise the middle chamber could be attributed to migration of NO_2^- from the cathode chamber through the AEM.

Overall, the increased concentrations of NH_4^+, NO_3^-, and NO_2^- in the middle chamber suggested that the cations (e.g., NH_4^+) migrated from the anode chamber to the middle chamber through the CEM. Similarly, the anions (e.g., NO_2^-, NO_3^-) moved from the cathode chamber to the middle chamber through the AEM. Although the recovery efficiencies of NH_4^+, NO_2^-, and NO_3^- could not be calculated since they were not contained in the wastewater initially, the results clearly demonstrated the recovery and concentration of ions (e.g., NH_4^+, NO_3^-, and NO_2^-) in the middle chamber (Table 1). The total nitrogen recovery efficiency reached 42%, the value was comparable to a previous method using a bio-electrochemical system coupled to a gas-permeable membrane unit (49%) [37] and higher than an 10-liter-scale microbial nutrient recovery system with membrane stack configuration (20%) [38].

3.2.4. PO_4^{3-} reduction and transfer

The PO_4^{3-} decreased from 0.90 to 0.48 ± 0.08 mg in the anode chamber and further reduced to < 0.10 mg in the cathode chamber. The removal efficiency was 99% and the removal rate was 5 $g\,m^{-3}\,d^{-1}$ (Fig. 4d and Table 1). The PO_4^{3-} could be reduced in the anode chamber by microbes which use P as a nutrient element [39]. The PO_4^{3-} could also be transferred from the cathode chamber to the middle chamber through the AEM under the effect of the electric field. As a result, the PO_4^{3-} increased from 0 to 0.33 ± 0.04 mg in the middle chamber with a recovery efficiency of 37% (Table 1). Additionally, the formation of struvite precipitates (Eq. (3)) under the alkali condition in the cathode chamber could be another reason that resulted in the decrease of PO_4^{3-} [40]. However, previous researches reported that precipitation of phosphate may cause problems for membranes and electrodes by obstructing the materials [41]. In the six-month operation of the RRMFC, no obvious precipitates or decrease of performance were observed, which could be due to the migration of NH_4^+ to the middle chamber. It is well-known that urea hydrolysis can induce struvite precipitation, attributing to the production of a large amount of NH_4^+ ions and the increase of pH [27]. However, the NH_4^+ ions migrated from the anode chamber into the middle chamber in the RRMFC, and thus the NH_4^+ concentration in the wastewater was largely reduced. Additionally, the pH did not increase too much in the RRMFC (6.00–7.90 for the effluents of the anode chamber and 8.10 ~ 8.90 for the effluents of the cathode chamber as shown in Table 1), which was not ideal for the formation reaction of struvite (pH > 9.00) [7].

3.2.5. SO_4^{2-} reduction and transfer

The SO_4^{2-} decreased from 1.70 to 0 mg in the anode chamber (Fig. 4d), meaning that SO_4^{2-} was reduced into S^{2-} or directly utilized by the microbes [42,43]. The S^{2-} could be re-oxidized to S or SO_4^{2-} in the cathode chamber in the presence of oxygen or nitrate [44]. As a result, the SO_4^{2-} increased from 0 to 0.04 ± 0.04 in the cathode chamber (Fig. 4d), and increased from 0 to 1.01 ± 0.15 mg in the middle chamber due to the transportation from the cathode chamber driven by the electric field. In total, the removal efficiency of SO_4^{2-} was 98% with a removal rate of 10 g m^{-3} d^{-1} and the recovery efficiency was 59% (Table 1).

3.2.6. Salinity

The salinity of the water was obtained by converting the conductivity to the corresponding NaCl concentration. In the anode chamber, the salinity increased from 24.60 to 46.04 ± 7.60 mg NaCl over one cycle (Fig. 4e). The reason is most likely due to the generation of NH_4^+ from urea, histidine and creatinine degradation. In the cathode chamber, the salinity decreased from 46.04 to 21.00 ± 6.10 mg NaCl at the end of a cycle (Fig. 4e), showing that anions migrated from the cathode chamber to the middle chamber through the AEM. In the middle chamber, the salinity increased from 0 to 47.65 ± 7.01 mg NaCl over one cycle (Fig. 4e), which could be attributed to the Cl^- migration from the cathode chamber as well as the Na^+ migration from the anode chamber. The removal efficiency of total salts was 15% with a removal rate of 21 g m^{-3} d^{-1} and the recovery efficiency was 33% (Table 1).

3.2.7. pH

The pH in the anode chamber was relatively stable in the range of 6.00–7.90 (Fig. 3f). This range was more beneficial for the growth of microbes compared to other urine-containing wastewater treatments usually with a larger increase of pH [45]. The reason to the small increase of the pH could be that the produced protons neutralized the alkalinity of NH_4^+ and also NH_4^+ migrated into the middle chamber. In the middle chamber, the pH increased from 7.20 to 7.90–8.50 (Fig. 3f). The pH in the cathode chamber increased from 6.00–7.90 to 8.10–8.90 (Fig. 3f), most likely due to the reduction of oxygen (Eq. (7)).

3.3. Working mechanisms of the RRMFC

The working mechanisms of the RRMFC haven been summarized in Fig. 5. In total, the RRMFC can not only remove urea, organics, and ions, but also recover N, P, and S nutrients and salts from the urine-containing wastewater. Detailly, in the anode chamber, urea was hydrolyzed into NH_3 and CO_2 through microbial processes (Eq. (1)) [18]. The produced NH_3 firsly dissolved in the water and formed NH_4^+ (Eq. (2)), which were further directly oxidized into NO_2^- and NO_3^- (Eq. (3)) or anaerobically oxidized to N_2 through the Anammox reaction (Eq. (4)) [35]. The organic matters (i.e., sodium acetate, creatinine, and histidine) were degraded by microbes into CO_2, NH_3, protons, electrons, and other intermediates (Eq. (5)). Most of the electrons produced from the oxidation reactions were transferred to the cathode to produce electricity. The rest electrons were used for reduction reactions such as reducing SO_4^{2-} to S^{2-} (Eq. (6)) [42,43]. Moreover, S compounds could be consumed by microbes as the growth nutrients [46], so were the N and P nutrients in the anode chamber.

At the cathode, oxygen diffused from the air to the cathode and was reduced by the electrons transferred from the anode to OH^- (Eq. (7)). In the cathode chamber, most of NH_4^+ produced from urea hydrolysis was oxidized by nitrification microbes into NO_2^- and NO_3^- (Eq. (8)) [30] or anaerobically oxidized to N_2 through the Anammox process (Eq. (4)) [35]. Besides, S^{2-} were reoxidized to S or SO_4^{2-} (Eq. (9)) [44], and Mg^{2+}, NH_4^+, and minimal PO_4^{3-} formed little struvite at the alkali pH condition in the cathode chamber (Eq. (10)).

Driven by the self-generated electric field, the cation ions (e.g., H^+, NH_4^+, K^+, Na^+, Ca^{2+}, Mg^{2+}) transferred from the anode chamber to the middle chamber through the CEM. At the same time, the anions (e.g., OH^-, SO_4^{2-}, PO_4^{3-}, NO_3^-, NO_2^-, Cl^-) transported from the cathode chamber to the middle chamber through the AEM. In contrast, the low mass out of NH_4^+ (3.2 mg), NO_3^- (0.6 mg), NO_2^- (0 mg), SO_4^{2-} (0.3 mg), PO_4^{3-} (0.04 mg), and salinity (0.01 mg) in the middle chamber of the control reactor under open circuit clearly revealed that the middle chamber hardly recovered nutrients and salts without the electric field.

The relatively large variability of the RRMFC could be due to the batch operation mode. The microbes in the system could be suffered from the exposure to air between cycles and affected by the fluctuations of substrate degradation rates and pH changes in each cycle, which was demonstrated by the obvious variation of electricity generation of the RRMFC (Fig. 2). A continuous flow mode would be better to obtain stable electricity generation and treatment performance.

$$(NH_2)_2CO + H_2O \rightarrow 2NH_3 + CO_2 \quad (1)$$

$$NH_3 + H_2O \rightarrow NH_4^+ + OH^- \quad (2)$$

$$NH_4^+ + 3H_2O \rightarrow NO_2^-/NO_3^- + 10H^+ + 8e^- \quad (3)$$

$$NH_4^+ + NO_2^- \rightarrow N_2 + 2H_2O \quad (4)$$

$$\text{Organic matters} \rightarrow CO_2 + NH_3 + \text{intermediates} + H^+ + e^- \quad (5)$$

$$SO_4^{2-} + 8H^+ + 8e^- \rightarrow S^{2-} + 4H_2O \quad (6)$$

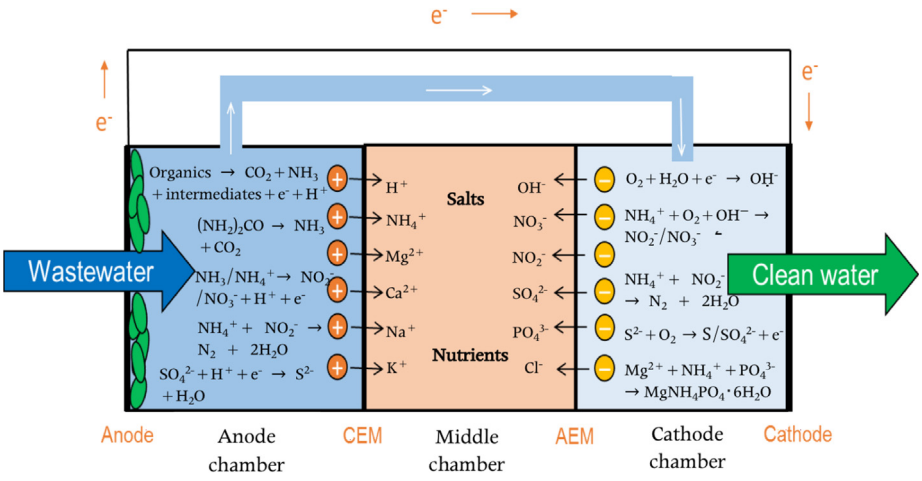

Fig. 5. Working mechanisms of the resource recovery microbial fuel cell (RRMFC) for wastewater treatment.

$$O_2 + 2H_2O + 4e^- \rightarrow 4OH^- \quad (7)$$

$$2NH_4^+ + 3O_2 \rightarrow 2NO_2^-/NO_3^- + 8H^+ \quad (8)$$

$$S^{2-} + 2O_2 \rightarrow S/SO_4^{2-} + 8e^- \quad (9)$$

$$Mg^{2+} + NH_4^+ + PO_4^{3-} + 6H_2O \rightarrow MgNH_4PO_4{\cdot}6H_2O \quad (10)$$

3.4. Outlook

The RRMFC effectively treated the urine-containing wastewater with various organic and inorganic pollutants without external energy input. It also efficiently recovered N, P, and S nutrients and salts from the wastewater. The COD removal efficiency of the RRMFC reached 97%, which was higher than previous results of a membrane-aerated and membrane-coupled bioreactor (M2BR) reactor (90%) [47]. The COD removal was also more successful than a microbial electrolysis cell system for ammonium recovery from urine in which the COD removal efficiency was only 46% [48]. Compared with the removal rate of six-stacked MFCs treating swine manure (1900 g COD m^{-3} d^{-1}) [49], the rate of 143 g COD m^{-3} d^{-1} in this study is low, most likely due to the lower initial organic concentration (1092 vs. 2470 mg L^{-1}). However, the COD removal rate of the RRMFC was similar to those of a granular activated carbon (GAC) module (100 g COD m^{-3} d^{-1}) [50] and a microbial fuel cell (181 g COD m^{-3} d^{-1}) [51].

The urea removal efficiency was 99% with a removal rate of 235 g m^{-3} d^{-1}, which was similar to previous methods for urine-containing wastewater treatment [30,41,52]. However, no separated urea hydrolysis was needed for the RRMFC. The urea hydrolysis was accelerated in the anode chamber by biological and microbial processes. Moreover, ammonium was directly recovered in the middle chamber through NH_4^+ migration driven by the self-generated electric field, which avoided to use the energy-intensive ammonia stripping process and the following costly acid trap of ammonia gas [53]. The total nitrogen recovery efficiency reached 42%, which was comparable to a previous method using a bio-electrochemical system coupled to a gas-permeable membrane unit (49%) [37], and higher than that of a scaled-up MEC (31%) with a applied 0.5 V voltage for urine wastewater treatment [54].

The PO_4^{3-} removal efficiency of the RRMFC was 99%, which was higher than those of previous studies that removed only 72–93% of PO_4^{3-} from urine-containing wastewater [45]. Although the PO_4^{3-} recovery efficiency was a little lower (37%) than that of previous systems integrating electrodialysis into electrochemical membrane bioreactor (45% and 65%) [55], the RRMFC requires no external energy consumption. The SO_4^{2-} removal efficiency of 98% was higher than those of MFCs (52–84%) [56]. The pH was stable around 6.00–8.00 in the anode chamber, which was superior to other processes for urine-containing wastewater treatment usually with a pH increase [57].

4. Conclusions

The RRMFC was very effective to remove organics and salts in the synthetic urine-containing water and simultaneously recover N, P, and S nutrients. The removal efficiency of urea reached 99% and the COD removal efficiency was high as 97%. Besides, the SO_4^{2-} and PO_4^{3-} removal efficiencies reached 98–99%. At the same time, the RRMFC recovered 42% of total nitrogen, 37% of PO_4^{3-}, 59% of SO_4^{2-}, and 33% of total salts. Moreover, no separate urea hydrolysis process, ammonium recovered by NH_4^+ migration driven by the self-generated electric field rather than the energy-intensive ammonia stripping, and a relative stable pH range for microbial growth, make this system attractive for urine-containing wastewater treatment.

Declaration of Competing Interest

None.

Acknowledgement

This research was funded by Louisiana Space Grant Consortium (LaSPACE), United States, Research Enhancement Award Program (AWDC-001589). The authors also thank Elizabeth Whiddon to edit the English.

Appendix A. Supplementary data

Supplementary data to this article can be found online at https://doi.org/10.1016/j.cej.2019.05.130.

References

[1] X. Zhang, E.A. Davidson, D.L. Mauzerall, T.D. Searchinger, P. Dumas, Y. Shen, Managing nitrogen for sustainable development, Nature 528 (2015) 51.
[2] Y. Park, S. Park, V.K. Nguyen, J. Yu, C.I. Torres, B.E. Rittmann, T. Lee, Complete nitrogen removal by simultaneous nitrification and denitrification in flat-panel air-cathode microbial fuel cells treating domestic wastewater, Chem. Eng. J. 316 (2017) 673–679.
[3] T.A. Larsen, W. Gujer, Separate management of anthropogenic nutrient solutions (human urine), Water Res. Technol. 34 (1996) 87–94.
[4] H. Mobley, R. Hausinger, Microbial ureases: significance, regulation, and molecular characterization, Microbiol. Rev. 53 (1989) 85–108.
[5] Q.-B. Zhao, J. Ma, I. Zeb, L. Yu, S. Chen, Y.-M. Zheng, C. Frear, Ammonia recovery from anaerobic digester effluent through direct aeration, Chem. Eng. J. 279 (2015) 31–37.
[6] S.G. Barbosa, L. Peixoto, B. Meulman, M.M. Alves, M.A. Pereira, A design of experiments to assess phosphorous removal and crystal properties in struvite precipitation of source separated urine using different Mg sources, Chem. Eng. J. 298 (2016) 146–153.
[7] P. Ledezma, P. Kuntke, C.J.N. Buisman, J. Keller, S. Freguia, Source-separated urine opens golden opportunities for microbial electrochemical technologies, Trends Biotechnol. 33 (2015) 214–220.
[8] M.E. Christiaens, K.M. Udert, J.B. Arends, S. Huysman, L. Vanhaecke, E. McAdam, K. Rabaey, Membrane stripping enables effective electrochemical ammonia recovery from urine while retaining microorganisms and micropollutants, Water Res. 150 (2019) 349–357.
[9] H. Kirchmann, S. Pettersson, Human urine-chemical composition and fertilizer use efficiency, Fert. Res. 40 (1994) 149–154.
[10] K. Udert, M. Wächter, Complete nutrient recovery from source-separated urine by nitrification and distillation, Water Res. 46 (2012) 453–464.
[11] B.E. Logan, Exoelectrogenic bacteria that power microbial fuel cells, Nat. Rev. Microbiol. 7 (2009) 375.
[12] H. Liu, R. Ramnarayanan, B.E. Logan, Production of electricity during wastewater treatment using a single chamber microbial fuel cell, Environ. Sci. Technol. 38 (2004) 2281–2285.
[13] X. Cao, X. Huang, P. Liang, K. Xiao, Y. Zhou, X. Zhang, B.E. Logan, A new method for water desalination using microbial desalination cells, Environ. Sci. Technol. 43 (2009) 7148–7152.
[14] H. Liu, S. Grot, B.E. Logan, Electrochemically assisted microbial production of hydrogen from acetate, Environ. Sci. Technol. 39 (2005) 4317–4320.
[15] I. Ieropoulos, J. Greenman, C. Melhuish, Urine utilisation by microbial fuel cells; energy fuel for the future, Phys. Chem. Chem. Phys. 14 (2012) 94–98.
[16] R.C. Tice, Y. Kim, Energy efficient reconcentration of diluted human urine using ion exchange membranes in bioelectrochemical systems, Water Res. 64 (2014) 61–72.
[17] J. De Paepe, S. Vlaeminck, K. Rabaey, F. Gòdia, P. Clauwaert, Bio-electrochemical pre-treatment and membrane aeration to intensify full nitrogen recovery for Spaceflight urine nitrification, 1st, Joint AgroSpace-MELiSSA workshop (2018).
[18] X. Chen, Y. Gao, D. Hou, H. Ma, L. Lu, D. Sun, X. Zhang, P. Liang, X. Huang, Z.J. Ren, The microbial electrochemical current accelerates urea hydrolysis for recovery of nutrients from source-separated urine, Environ. Sci. Technol. Lett. 4 (2017) 305–310.
[19] W. Pronk, M. Biebow, M. Boller, Electrodialysis for recovering salts from a urine solution containing micropollutants, Environ. Sci. Technol. 40 (2006) 2414–2420.
[20] S. Giannakis, B. Androulaki, C. Comninellis, C. Pulgarin, Wastewater and urine treatment by UVC-based advanced oxidation processes: implications from the interactions of bacteria, viruses, and chemical contaminants, Chem. Eng. J. 343 (2018) 270–282.
[21] Y. Feng, Q. Yang, X. Wang, B.E. Logan, Treatment of carbon fiber brush anodes for improving power generation in air-cathode microbial fuel cells, J. Power Sources 195 (2010) 1841–1844.
[22] W. Yang, W. He, F. Zhang, M.A. Hickner, B.E. Logan, Single-step fabrication using a phase inversion method of poly(vinylidene fluoride) (PVDF) activated carbon air cathodes for microbial fuel cells, Environ. Sci. Technol. Lett. 1 (2014) 416–420.
[23] X. Zhu, M.D. Yates, M.C. Hatzell, H. Ananda Rao, P.E. Saikaly, B.E. Logan, Microbial

community composition is unaffected by anode potential, Environ. Sci. Technol. 48 (2014) 1352–1358.
[24] A.P.H. Association, A.W.W. Association, W.P.C. Federation, W.E. Federation, Standard methods for the examination of water and wastewater, Am. Public Health Assoc. (1915).
[25] G.W. Watt, J.D. Chrisp, Spectrophotometric method for determination of urea, Anal. Chem. 26 (1954) 452–453.
[26] B.E. Logan, B. Hamelers, R. Rozendal, U. Schröder, J. Keller, S. Freguia, P. Aelterman, W. Verstraete, K. Rabaey, Microbial fuel cells: methodology and technology, Environ. Sci. Technol. 40 (2006) 5181–5192.
[27] C. Santoro, C. Arbizzani, B. Erable, I. Ieropoulos, Microbial fuel cells: from fundamentals to applications. A review, J. Power Sources 356 (2017) 225–244.
[28] K.M. Udert, T.A. Larsen, M. Biebow, W. Gujer, Urea hydrolysis and precipitation dynamics in a urine-collecting system, Water Res. 37 (2003) 2571–2582.
[29] F. Zeng, Q. Zhao, W. Jin, Y. Liu, K. Wang, D.-J. Lee, Struvite precipitation from anaerobic sludge supernatant and mixed fresh/stale human urine, Chem. Eng. J. 344 (2018) 254–261.
[30] F. Zhang, Z. He, Simultaneous nitrification and denitrification with electricity generation in dual-cathode microbial fuel cells, J. Chem. Technol. Biot. 87 (2012) 153–159.
[31] T.-L. Zhao, H. Li, Y.-R. Huang, Q.-Z. Yao, Y. Huang, G.-T. Zhou, Microbial mineralization of struvite: salinity effect and its implication for phosphorus removal and recovery, Chem. Eng. J. 358 (2019) 1324–1331.
[32] H.R. Mackey, G. Rey Morito, T. Hao, G.H. Chen, Pursuit of urine nitrifying granular sludge for decentralised nitrite production and sewer gas control, Chem. Eng. J. 289 (2016) 17–27.
[33] S. Giannakis, I. Hendaoui, M. Jovic, D. Grandjean, L.F. De Alencastro, H. Girault, C. Pulgarin, Solar photo-Fenton and UV/H2O2 processes against the antidepressant Venlafaxine in urban wastewaters and human urine. Intermediates formation and biodegradability assessment, Chem. Eng. J. 308 (2017) 492–504.
[34] L. Lu, D. Xing, N. Ren, Pyrosequencing reveals highly diverse microbial communities in microbial electrolysis cells involved in enhanced H2 production from waste activated sludge, Water Res. 46 (2012) 2425–2434.
[35] I. Schmidt, E. Bock, Anaerobic ammonia oxidation with nitrogen dioxide by Nitrosomonas eutropha, Arch. Microbiol. 167 (1997) 106–111.
[36] Z. Chu, K. Wang, X. Li, M. Zhu, L. Yang, J. Zhang, Microbial characterization of aggregates within a one-stage nitritation–anammox system using high-throughput amplicon sequencing, Chem. Eng. J. 262 (2015) 41–48.
[37] M. Rodríguez Arredondo, P. Kuntke, A. Ter Heijne, H.V.M. Hamelers, C.J.N. Buisman, Load ratio determines the ammonia recovery and energy input of an electrochemical system, Water Res. 111 (2017) 330–337.
[38] X. Chen, H. Zhou, K. Zuo, Y. Zhou, Q. Wang, D. Sun, Y. Gao, P. Liang, X. Zhang, Z.J. Ren, Self-sustaining advanced wastewater purification and simultaneous in situ nutrient recovery in a novel bioelectrochemical system, Chem Eng. J. 330 (2017) 692–697.
[39] X. Mei, D. Xing, Y. Yang, Q. Liu, H. Zhou, C. Guo, N. Ren, Adaptation of microbial community of the anode biofilm in microbial fuel cells to temperature, Bioelectrochemistry 117 (2017) 29–33.
[40] H.B. Liu, F. Leng, Y.L. Guan, Y.Y. Yao, Y.H. Li, S.Y. Xu, Simultaneous pollutant removal and electricity generation in a combined ABR-MFC-MEC system treating fecal wastewater, Water Air Soil Poll. 228 (2017).
[41] M.R. Arredondo, P. Kuntke, A. Jeremiasse, T. Sleutels, C. Buisman, A. Ter Heijne, Bioelectrochemical systems for nitrogen removal and recovery from wastewater, Environ. Sci.: Water Res. Technol. 1 (2015) 22–33.
[42] M. Yang, Y. Zhong, B. Zhang, J. Shi, X. Huang, Y. Xing, L. Su, H. Liu, A.G.L. Borthwick, Enhanced sulfide removal and bioelectricity generation in microbial fuel cells with anodes modified by vertically oriented nanosheets, Environ. Technol. 1–10 (2018).
[43] W. Habermann, E. Pommer, Biological fuel cells with sulphide storage capacity, Appl. Microbiol. Biotechnol. 35 (1991) 128–133.
[44] H. Lu, H. Huang, W. Yang, H.R. Mackey, S.K. Khanal, D. Wu, G.H. Chen, Elucidating the stimulatory and inhibitory effects of dissolved sulfide on sulfur-oxidizing bacteria (SOB) driven autotrophic denitrification, Water Res. 133 (2018) 165–172.
[45] I. Merino-Jimenez, V. Celorrio, D.J. Fermin, J. Greenman, I. Ieropoulos, Enhanced MFC power production and struvite recovery by the addition of sea salts to urine, Water Res. 109 (2017) 46–53.
[46] W. Li, Q. Niu, H. Zhang, Z. Tian, Y. Zhang, Y. Gao, Y.-Y. Li, O. Nishimura, M. Yang, UASB treatment of chemical synthesis-based pharmaceutical wastewater containing rich organic sulfur compounds and sulfate and associated microbial characteristics, Chem. Eng. J. 260 (2015) 55–63.
[47] R.D. Chen, M.J. Semmens, T.M. LaPara, Biological treatment of a synthetic space mission wastewater using a membrane-aerated, membrane-coupled bioreactor (M2BR), J. Ind. Microbiol. Biotechnol. 35 (2008) 465–473.
[48] P. Kuntke, T.H.J.A. Sleutels, M. Saakes, C.J.N. Buisman, Hydrogen production and ammonium recovery from urine by a Microbial Electrolysis Cell, Int. J. Hydrog. Energy 39 (2014) 4771–4778.
[49] A. Vilajeliu-Pons, S. Puig, I. Salcedo-Dávila, M. Balaguer, J. Colprim, Long-term assessment of six-stacked scaled-up MFCs treating swine manure with different electrode materials, Environ. Sci.: Water Res. 3 (2017) 947–959.
[50] T.W. Rogers, T.S. Rogers, M.H. Stoner, K.L. Sellgren, B.J. Lynch, A.A. Forbis-Stokes, B.R. Stoner, B.T. Hawkins, A granular activated carbon/electrochemical hybrid system for onsite treatment and reuse of blackwater, Water Res. 144 (2018) 553–560.
[51] M. Rodríguez Arredondo, P. Kuntke, A.W. Jeremiasse, T.H.J.A. Sleutels, C.J.N. Buisman, A. Ter Heijne, Bioelectrochemical systems for nitrogen removal and recovery from wastewater, Environ. Sci.: Water Res. Technol. 1 (2015) 22–33.
[52] W.T. Tang, J. Dai, R. Liu, G.H. Chen, Microbial ureolysis in the seawater-catalysed urine phosphorus recovery system: kinetic study and reactor verification, Water Res. 87 (2015) 10–19.
[53] W.A. Tarpeh, J.M. Barazesh, T.Y. Cath, K.L. Nelson, Electrochemical stripping to recover nitrogen from source-separated urine, Environ. Sci. Technol. 52 (2018) 1453–1460.
[54] P. Zamora, T. Georgieva, A. Ter Heijne, T.H. Sleutels, A.W. Jeremiasse, M. Saakes, C.J. Buisman, P. Kuntke, Ammonia recovery from urine in a scaled-up Microbial Electrolysis Cell, J Power Sources 356 (2017) 491–499.
[55] Y.K. Wang, Y.K. Geng, X.R. Pan, G.P. Sheng, In situ utilization of generated electricity for nutrient recovery in urine treatment using a selective electrodialysis membrane bioreactor, Chem. Eng. Sci. 171 (2017) 451–458.
[56] Y. Zhang, I. Angelidaki, Submersible microbial fuel cell sensor for monitoring microbial activity and BOD in groundwater: focusing on impact of anodic biofilm on sensor applicability, Biotechnol. Bioeng. 108 (2011) 2339–2347.
[57] L. Wang, B. Xie, N. Gao, B. Min, H. Liu, Urea removal coupled with enhanced electricity generation in single-chambered microbial fuel cells, Environ. Sci. Pollut. Res. Int. 24 (2017) 20401–20408.